

Binding of an antimicrobial peptide to bacterial cells: interaction with different species, strains and cellular components.

F. Savini,^{1,*} M.R. Loffredo,^{2,*} C. Troiano,¹ S. Bobone,¹ N. Malanovic,³ T. O. Eichmann,⁴ L. Caprio,¹ V. C. Canale,¹ Y. Park,⁵ M. L. Mangoni,^{2,+} L. Stella^{1,+}

¹ Department of Chemical Science and Technologies, University of Rome Tor Vergata, Rome, Italy

² Laboratory affiliated to Pasteur Italia-Fondazione Cenci Bolognetti, Department of Biochemical Sciences, Sapienza University of Rome, Rome, Italy

³ Institute of Molecular Biosciences, Biophysics Division, Karl-Franzens University Graz, Graz, Austria.

⁴ Institute of Molecular Biosciences, Karl-Franzens University Graz and Center for Explorative Lipidomics, BioTechMed-Graz, Graz, Austria

⁵ Department of Biomedical Science, College of Natural Science, Chosun University, Gwangju, Republic of KOREA

* These authors contributed equally

+ to whom correspondence should be addressed

marialuisa.mangoni@uniroma1.it, stella@uniroma2.it

Abstract

Antimicrobial peptides (AMPs) selectively kill bacteria by disrupting their cell membranes, and are promising compounds to fight drug-resistant microbes. Biophysical studies on model membranes have characterized AMP/membrane interactions and the mechanism of bilayer perturbation, showing that accumulation of cationic peptide molecules in the external leaflet leads to the formation of pores ("carpet" mechanism). However, similar quantitative studies on real cells are extremely limited. Here, we investigated the interaction of the dansylated PMAP23 peptide (DNS-PMAP23) with a Gram-positive bacterium, showing that 10^7 bound peptide molecules per cell are needed to kill it. This result is consistent with our previous finding for Gram-negative strains, where a similar high threshold for killing was determined, demonstrating the general relevance of the carpet model for real bacteria. However, in the case of the Gram-positive strain, this number of molecules even exceeds the total surface available on the bacterial membrane. The high affinity of DNS-PMAP23 for the anionic teichoic acids of the Gram-positive cell wall, but not for the lipopolysaccharides of Gram-negative bacteria, provides a rationale for this finding. To better define the role of anionic lipids in peptide/cell association, we studied DNS-PMAP23 interaction with *E. coli* mutant strains lacking phosphatidylglycerol and/or cardiolipin. Surprisingly, these strains showed a peptide affinity similar to that of the wild type. This finding was rationalized by observing that these bacteria have an increased content of other anionic lipids, thus maintaining the total membrane charge essentially constant. Finally, studies of DNS-PMAP23 association to dead bacteria showed an affinity an order of magnitude higher compared to that of live cells, suggesting strong peptide binding to intracellular components that become accessible after membrane perturbation. This effect could play a role in population resistance to AMP action, since dead bacteria could protect the surviving cells by sequestering significant amounts of peptide molecules. Overall, our data indicate that quantitative studies of peptide association to bacteria can lead to a better understanding of the mechanism of action of AMPs.

Introduction

The emergence and diffusion of drug resistant bacteria (germs that are not susceptible to several or even all the currently available antibiotics) is one of the greatest health challenges of our time. We are currently at risk of losing the transformative medical progress made possible by antibiotic drugs, such as the easy treatment of deadly infectious diseases, surgery, transplants or anticancer chemotherapy. The latest report on antibiotic resistance by the US Centers for Disease Control and Prevention [CDC 2019] warns us that we are already living in a post-antibiotic era: in the US alone, one person is killed by drug resistant microbes every 15 minutes. Global deaths by “superbugs”, as these bacteria are called, are currently estimated at more than 700,000 per year, but this figure could increase to 10 millions by 2050 if no action is taken [UN-IACG 2019]. New drugs against resistant bacteria are severely needed.

Antimicrobial peptides (AMPs, often also called host defense peptides, or HDPs) are an important component of our innate defense system [Zasloff 2019]. These molecules have multiple functions, including immunomodulatory roles [van der Does 2019], but they are mainly bactericidal. Thousands of different natural AMPs are currently known: their sequences do not show any conserved motif, but they all share some properties. They are usually short, cationic and amphipathic [Bobone 2019]. Most AMPs act by binding to bacterial membranes and making them permeable, through the formation of pores [Matsuzaki 2019]. Since this mechanism of action does not involve any specific protein target, development of bacterial resistance is difficult and AMPs have a wide spectrum of activity and are effective also against resistant strains [Zasloff 2019].

AMPs have the additional desirable property of being moderately selective, i.e. they are active against bacteria at concentrations where their toxicity to the host cells is negligible. This property is attributed mostly to the fact that microbial membranes display lipids with negatively charged phospholipid headgroups (phosphatidylglycerol or PG, cardiolipin or CL) on their surface, while in the membranes of eukaryotic cells anionic lipids are segregated to the inner leaflet [Bobone 2019]. Consistently, AMPs interact more strongly with anionic than with neutral artificial membranes, due to their cationic nature [Bobone 2019].

Studies on model membranes led to the proposal of several mechanisms of pore formation by AMPs [Matsuzaki 2019], but the most widely applicable model is based on accumulation of peptides on the outer leaflet of the bilayer, perturbation of its surface tension and formation of pores or defects. In artificial vesicles, the bound peptide to lipid ratios necessary for perturbation of membrane permeability are typically of the order of 1/10, which corresponds to complete coverage of the bilayer [Melo 2009]. For this reason, this mechanism has been termed the “carpet” model [Gazit 1996].

Based on the above discussion, it is clear that peptide binding to bacterial membranes is a major determinant of AMP activity and selectivity. However, while peptide/membrane association is easily determined in biophysical studies on model bilayers, quantification of this phenomenon in real cells has received very limited attention. Recently, several groups, including ours, have tried to bridge the gap between microbiological studies (where peptide activity is determined, but the amount of peptide associated to the cells is unknown) and biophysical studies on extremely simplified model systems [Roversi 2014, Starr 2016, Savini 2017, Savini 2018, Snoussi 2018, Zhu 2019, Wu 2019]. In particular, we developed experimental conditions suitable for the determination of both the bactericidal activity and peptide/cell association, in a minimal medium where the bacteria are vital but do not multiply and thus the cell density is well-defined [Roversi 2014]. These studies focused on Gram-negative *E. coli* cells and on DNS-PMAP23, a fluorescently labeled analogue of PMAP-23, a typical cationic AMP belonging to the cathelicidin family and acting according to the carpet mechanism in model membranes [Bocchinfuso 2009, Orioni 2009]. Thanks to these data, we determined that at the minimum bactericidal concentration (MBC) 10^7 DNS-PMAP23 molecules are bound to each cell. This number showed for the first time that the high membrane coverage necessary for pore formation in liposomes is reached at the MBC in real bacteria, and provided a strong support to the carpet model of membrane perturbation as the mechanism of action in real cells, at least for our peptide. Interestingly, the few other available studies of peptide binding to *E. coli* cells indicate that this order of magnitude is common to other AMPs [Savini 2018, Starr 2016, Tran 2002, Steiner 1988]. However, this interesting finding opened more questions than it answered [Savini 2018].

One crucial issue is whether the behavior, now observed only for a very limited number of AMPs and bacterial strains, is relevant also for other systems. In particular, to the best of our knowledge, only one experiment on Gram-positive bacteria has been reported, on the association of Cecropin A to *B. megaterium* [Steiner 1988]. However, this bacterium is rather atypical due to its unusual size, as it can reach up to 4 μm of length. Considering the great differences in the cellular envelopes between Gram-negative and Gram-positive bacteria, further studies focusing on Gram-positives are warranted.

The very high accumulation of peptides needed for killing begs the question of where all these molecules are located in a bacterial cell. A related ongoing debate also regards the role of the saccharidic portion of lipopolysaccharide (LPS) and of cell wall components (particularly of Gram-positive bacterial strains) in the mechanism of action of AMPs. Do these components facilitate the activity of AMPs, by guiding their access to the plasma membrane, or do they rather inhibit their action by sequestering peptide molecules and reducing their effective concentration? Reviews on this topic by Prof. Karl Lohner outlined this issue and urged for further affinity studies of AMPs towards LPS and cell wall components, inspiring us to pursue our investigations further [Malanovic 2016, Brandenburg 2016].

Finally, three microscopy studies, published in the last year, reported an accumulation of AMPs inside the bacterial cells, after membrane permeabilization [Snoussi 2018, Zhu 2019, Wu 2019]. This phenomenon might be just the consequence of the accessibility of internal molecules and components as additional binding partners [Snoussi 2018, Wu 2019], or it could contribute to bacterial killing [Zhu 2019]. In any case, peptide sequestration by dead cells might help other bacteria to survive to AMP action, by reducing the available peptide concentration [Snoussi 2018, Zhu 2019, Wu 2019].

With the goal of addressing these questions, we have investigated the interaction of DNS-PMAP23 with a Gram-positive bacterium, with lipoteichoic acids, with bacterial cells in which specific mutations caused variations in the LPS structure or in the lipid composition of the cytoplasmic membrane, and with live and dead bacterial cells.

Materials and Methods

Materials

DNS-PMAP23 (Dansyl-RIIDLLWRVRRPQKPKFVTWVVR-NH₂) was purchased from AnyGen Co. (Gwangju, South Korea). Bacterial culture media were purchased from Oxoid (Basingstoke, UK), 96-well plates were from Falcon (Franklin Lakes, NJ, USA). Lipoteichoic acid (LTA) was purchased from Sigma Aldrich (ST Louis, Missouri, USA).

Microorganisms

The following strains were used for the antimicrobial assays: the Gram-negative bacteria *Escherichia coli* ATCC 25922, D21 and *E. coli* D21f2, a D21 mutant in genes *rfa-1* and *rfa-31* (formerly called *lpsA1* and *lpsD31*) lacking of the O-antigen and oligosaccharide core [Mangoni 2009, Farnaud 2004, Boman 1975], *E. coli* MG1655 (K-12), and its mutant strains BKT12 (lacking the *clsABC* genes required for cardiolipin (CL) biosynthesis) and BKT29 (lacking the *pgsA* gene, in addition to the *clsABC* and *ymdB* genes; *pgsA* encodes a phosphatidylglycerol phosphate synthase, which catalyzes PG synthesis, from phosphatidic acid (PA) [Tan 2012, Oliver 2014, Agrawal 2019]; the Gram-positive bacterium *Staphylococcus epidermidis* ATCC 12228. Strains BKT12 and BKT29 were a kind gift by Prof. J. C. Weisshaar (University of Wisconsin-Madison).

Antimicrobial assays

-Bactericidal activity

With the goal of determining the bactericidal activity of DNS-PMAP23, in the presence of a well-defined number of *S. epidermidis* cells, the following assay was developed, similarly to our previous studies on *E. coli* [Roversi 2014]. *S. epidermidis* was grown in Luria Bertani (LB) medium at 37 °C under mild agitation (200 rpm), to a mid-logarithmic phase. After centrifugation at 1,400 x g for 10 min and washing for three times, the bacterial culture was resuspended in buffer A (5 mM HEPES, 110 mM KCl, 15 mM glucose, pH 7.3), a minimal culture medium where bacteria are vital, but do not multiply, thus maintaining a constant number of live cells in the time-frame of the experiments (Figure S1).

$(4.5 \pm 0.5) \times 10^8$ colony forming units (CFU)/mL were mixed with different concentrations of DNS-PMAP23 (final volume of 100 μ L). The content of peptide solvent (methanol) was 5% in all final samples, and was included also in controls, run without peptide. Similarly to our previous studies, the relatively high cell density employed in this assay ensured that bactericidal peptide concentrations were in the micromolar range, suitable for the cell binding experiments (see below). After 120 min incubation with the peptide at 37 °C, under moderate agitation (800 rpm, to avoid the formation of bacterial clumps and/or their precipitation at the bottom of the test tube), aliquots (5 μ L) were appropriately diluted in buffer A and spread onto LB-agar plates for counting. After overnight incubation at 37 °C, the number of CFU was determined [Luca 2013; Di Grazia 2015; Marcellini 2009]. The number of surviving bacterial cells was reported as percentage compared to the control.

-Determination of minimum inhibitory concentration (MIC)

In addition to the bactericidal activity, MIC (the most commonly used measure of antimicrobial peptide activity) was determined, too, for comparison, by adapting the microbroth dilution method, using sterile 96-wells plates. Aliquots (50 μ L) of bacteria in mid-logarithmic phase at a concentration of 2×10^6 CFU/mL in culture medium (Mueller-Hinton, MH) were added to 50 μ L of MH broth containing the peptide in serial 2-fold dilutions in methanol (at a 5% final solvent concentration). The MIC was expressed as the minimum concentration of peptide at which 100% inhibition of microbial growth is visually observed after 16-18 h of incubation at 37 °C [Merlino 2017, Grieco 2013, Casciaro 2019].

Preparation of dead bacteria

To measure peptide association to dead bacterial cells, bacteria grown to the mid-logarithmic phase were centrifuged at 1,400 x g for 10 min and washed eight times; afterwards, they were resuspended in buffer A at a final cell density of 6×10^9 CFU/mL. Two mL were then sonicated with Sonic Vibra Cell (80 % amplitude 10 sec on and 10 sec off pulses for 10 min, under ice) to kill bacteria (as demonstrated by CFU counting).

Peptide association to bacteria and LTA.

Bacterial cells were grown, collected and washed as described above and resuspended in buffer A (*S. epidermidis* and *E. coli* ATCC 25922) or buffer B (phosphate buffered saline (PBS) supplemented with 15 mM glucose, for *E. coli* D21, D21f2, BKT12, BKT29, and K-12 MG1655) at a final cell density of 6×10^9 CFU/ml. Measurement samples were maintained at 37 °C, while stock cell suspensions at 25 °C. As indicated by colony counts at different times, these conditions ensured a stable number of vital cells for at least 6 hours at 25 °C or 2 hours at 37 °C (*i.e.* more than the time required for our experiments).

A fixed peptide concentration (in buffer A or B) was titrated with increasing concentrations of bacterial cells. After each addition, the fluorescence spectra were recorded repeatedly until no further changes were observed (about 5-10 minutes).

Experiments were performed with a HORIBA (Edison, NJ) FluoroMax-4 fluorimeter, with $\lambda_{exc.}=340$ nm, integration time 0.4 s, bandwidths of 1.5–2 nm in excitation and emission, respectively, when a peptide concentration of 10 μ M or 50 μ M was used, or 3–5 nm for a peptide concentration of 2 μ M. The temperature was controlled with a thermostatted cuvette holder set at 37 °C for all experiments.

Control experiments to check for possible effects of *S. epidermidis* sample turbidity on the fluorescence signal were performed by repeating the same titration (using the same conditions of the 50 μ M DNS-PMAP23 experiments) with dansylamide.

The fraction of peptide associated to membranes was calculated from the fluorescence intensity at 515 nm (F), according to the following equation [Bocchini 2011]:

$$f = \frac{F - F_M}{F_M - F_W}$$

where F_W and F_M represent the fluorescence intensities of the peptide in water and in the membrane, respectively. The latter was determined by fitting directly the F vs $[Cells]$ titration with the following phenomenological Hill equation:

$$F = F_W + (F_M - F_W) \frac{([Cells]/C_{50})^n}{1 + ([Cells]/C_{50})^n}$$

where C_{50} represents an apparent dissociation constant, or the cell concentration causing half maximal binding, $[Cells]$ is the concentration of bacterial cells and n is a parameter to take into account the sigmoidal shape of the curve [Roversi 2014].

LTA was dissolved in ultrapure water at the concentration of 5 mg/ml. The stock solution or a tenfold dilution was used for the binding experiment. DNS-PMAP23 (10 μ M in buffer A) was titrated with increasing amounts of LTA, in the same conditions used for bacterial association experiments. In this case, too, the fraction of bound peptide was calculated from the intensity of the dansyl moiety at 515 nm.

Zeta-potential measurements

Peptide/cell association was characterized also by measurements of zeta potential [Freire 2011]. Mid-logarithmic growing cells were diluted to 1×10^7 CFU/mL in HEPES buffer (10 mM HEPES, 140 mM NaCl, pH 7.4) and exposed to different peptide concentrations. After 5 min incubation at room temperature (RT), they were measured on a Zetasizer (Zetasizer NANO, Malvern Instruments, Herrenberg, Germany) according to previously published methods [Pérez-Peinado 2018, Huber 2019].

Lipid analysis

The membrane lipid composition of mutant *E. coli* strains BKT12 and BKT29, and of the parent strain MG1655 (K-12), was characterized by lipid analysis. Bacteria were grown overnight at 37 °C in MH broth and then inoculated at 0.05 optical density (OD) to a fresh MH broth. The growth was stopped after 4 h, corresponding to the mid-logarithmic growth phase, and cells were collected by centrifugation. Approximately 10 mL of a 1 OD cell suspension were washed twice with phosphate buffered saline, pH=7 and kept at -80 °C, until further preparation steps.

Bacterial pellets were extracted according to Matyash et al. [Matyash 2008] in 700 µL methyl-tert-butyl ether (MTBE)/methanol (3/1, v/v), containing 500 pmol butylated hydroxytoluene, 1% acetic acid, and internal standards (IS; 50 pmol of 1,2-diheptadecanoyl-*sn*-glycero-3-phosphocholine; Larodan, Solna, Sweden). Total lipid extraction was performed under constant shaking for 30 min at room temperature (RT). After addition of 40 µL dH₂O (140 µL total aqueous phase) and further incubation for 30 min at RT, samples were centrifuged at 1,000 × g for 15 min. Afterwards, 500 µL of the upper, organic phase were collected and dried under a stream of nitrogen. Lipids were re-dissolved in 500 µL MTBE/methanol (3/1, v/v) and diluted in 2-propanol/methanol/dH₂O (7/2.5/1, v/v/v) for UHPLC-qTOF analysis. Chromatographic separation was performed on a 1290 Infinity II LC system (Agilent, Santa Clara, CA, USA) equipped with a Luna omega C18 column (2.1x50 mm, 1.6 µm; Phenomenex, Torrance, CA, USA), running a 20 min linear gradient from 55% solvent A (H₂O; 10 mM ammonium acetate, 0.1% formic acid, 8 µM phosphoric acid) to 100% solvent B (2-propanol; 10 mM ammonium acetate, 0.1% formic acid, 8 µM phosphoric acid). The column compartment was kept at 50 °C. A 6560 Ion Mobility Q-TOF mass spectrometer (Agilent, Santa Clara, CA, USA), equipped with Dual AJS ESI source, was used for detection of lipids in positive Q-TOF mode. The MassHunter data acquisition software (B.09, Agilent, Santa Clara, CA, USA) was used for data acquisition. Lipids were manually identified and lipid feature extraction was performed using MassHunter Profinder (V.10, Agilent, Santa Clara, CA, USA). Data were normalized for recovery and extraction efficacy by calculating analyte/IS ratios (arbitrary units, A.U.) and expressed as A.U./µg protein. They are reported after normalization to the lipid content of the wild type (WT) strain.

Results and Discussion

Peptide association to Gram-positive and Gram-negative bacteria: general validity of the carpet model

Extending our previous studies on *E. coli* [Roversi 2014, Savini 2017], we investigated the interaction of DNS-PMAP23 with the Gram-positive bacterium *S. epidermidis*.

MIC of DNS-PMAP23 against the Gram-negative *E. coli* (ATCC 25922) and the Gram-positive *S. epidermidis* (ATCC 12228) were comparable (32 μ M and 16 μ M, respectively), in agreement with previous reports on the activity of the unlabeled peptide against the two bacterial classes [Zanetti 1994, Kang 1999, Veldhuizen 2017]. However, the MIC assay was not suitable for our goal of determining the number of cell-bound peptide molecules needed for bacterial killing. By definition, the MIC assay requires a medium in which bacteria grow, while we needed a well-defined and stable cell density. In addition, the culture broth used in the MIC assay (Mueller–Hinton broth, MH) can sequester a significant amount of peptide and interfere with spectroscopic measurements [Roversi 2014].

Similarly to our previous studies [Roversi 2014, Savini 2017], we used a minimal culture medium (5 mM HEPES, 110 mM KCl, 15 mM glucose, pH 7.3) to obtain that *S. epidermidis* cells remained vital, but at a constant cell density, for the time needed for our experiments. As shown in Figure S1, the cell density stayed constant for at least 6 h for the 6×10^9 CFU/mL stock solution at room temperature (where it was stored) and for at least 2 hours at 37 °C for a cell density of 4.5×10^8 , i.e. under conditions typically used in our binding and bacterial killing experiments. All our experiments were performed in these time-frames; therefore, we had a well-defined cell density in all our studies. Furthermore, this medium did not interfere with the spectroscopic measurements.

To measure the antimicrobial activity of DNS-PAMP23 in the minimal medium, a bacterial killing assay was performed. These experiments were carried out in the presence of $(4.5 \pm 0.5) \times 10^8$ cells/mL at 37 °C (Figure 1), as this density ensured that the MBC fell in the micromolar range needed for the spectroscopic binding measurements. Indeed, under these conditions, the bactericidal activity of DNS-PMAP23 started at $[P]_{\text{tot}} = 2.0 \mu\text{M}$ (killing $9 \pm 2\%$), while $>99.9\%$ bacterial killing was attained at $[P]_{\text{tot}} = 50 \mu\text{M}$ (Figure 2). Therefore, we selected these two peptide concentration values, and 10 μM (killing $91 \pm 1\%$) for evaluating DNS-PMAP23 association to the bacterial cells.

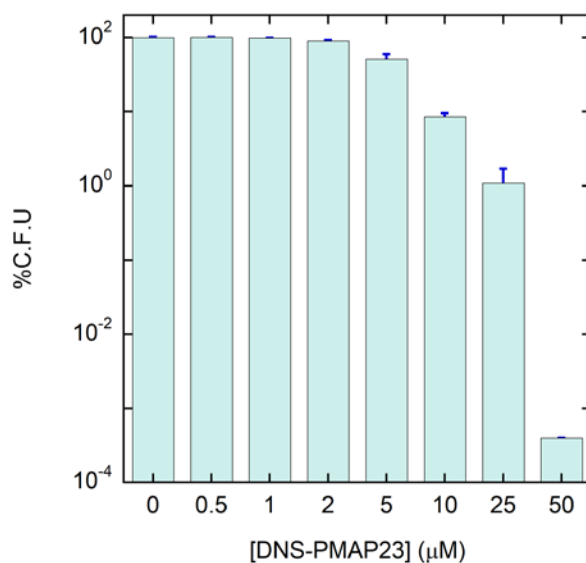


Figure 1. Microbicidal activity of DNS-PMAP23 on *S. epidermidis* cells.

Survival of *S. epidermidis* cells (starting cell density, 4.5×10^8 CFU/mL) after 2h of incubation at 37° C with different concentrations of DNS-PMAP23.

We performed experiments of peptide binding to bacterial membranes by fluorescence spectroscopy. PMAP-23 is intrinsically fluorescent [Orioni 2009], but the introduction of an extrinsic dansyl fluorophore at the N-terminus of DNS-PMAP23 was necessary to obtain a signal not overlapping to the intrinsic fluorescence of bacterial proteins [Bobone 2014; Bortolotti 2016]. Although a slight perturbation of the peptide behavior by the fluorophore is possible [Roversi 2014, Savini 2017], by performing binding and killing experiments under the same conditions (temperature and medium) of the MBC assays, we ensured that the probe affected both datasets in the same way, so that it could be factored out.

Titration of DNS-PMAP23 with increasing densities of *S. epidermidis* cells caused an increase in the fluorescence intensity and a blue shift of the maximum of the emission spectrum, as previously observed with *E. coli* [Roversi 2014]. These are distinctive features of dansyl insertion in an apolar, relatively rigid environment and thus indicate association to bacterial membranes. By contrast, performing a similar titration with the dansyl analogue dansylamide (which does not bind to membranes [Roversi 2014]) did not cause significant variations in the fluorescence signal, ruling out possible artifacts due to sample turbidity, caused by the bacterial cells in suspension (Figure 2).

We calculated the fraction of peptide bound to bacterial cells from the variation of fluorescence intensity at a fixed wavelength (515 nm) (Figure 3). Apparent dissociation constants determined from these curves (i.e. the concentration of half maximal binding, C_{50}) are reported in Table 1. Their order of magnitude is comparable to the values previously determined for *E. coli* [Roversi 2014, Savini 2017]. The dependence of the curves on peptide concentration is significantly more marked than in the case of *E. coli* cells [Roversi 2014, Savini 2017]. This finding is compatible with an association process where electrostatic interactions play a significant role, rather than with an ideal water/membrane partition equilibrium [Seelig 2004], and is consistent with the fact that the content of anionic lipids in Gram-positive bacterial membranes is significantly higher than in Gram-negatives [Bobone 2019].

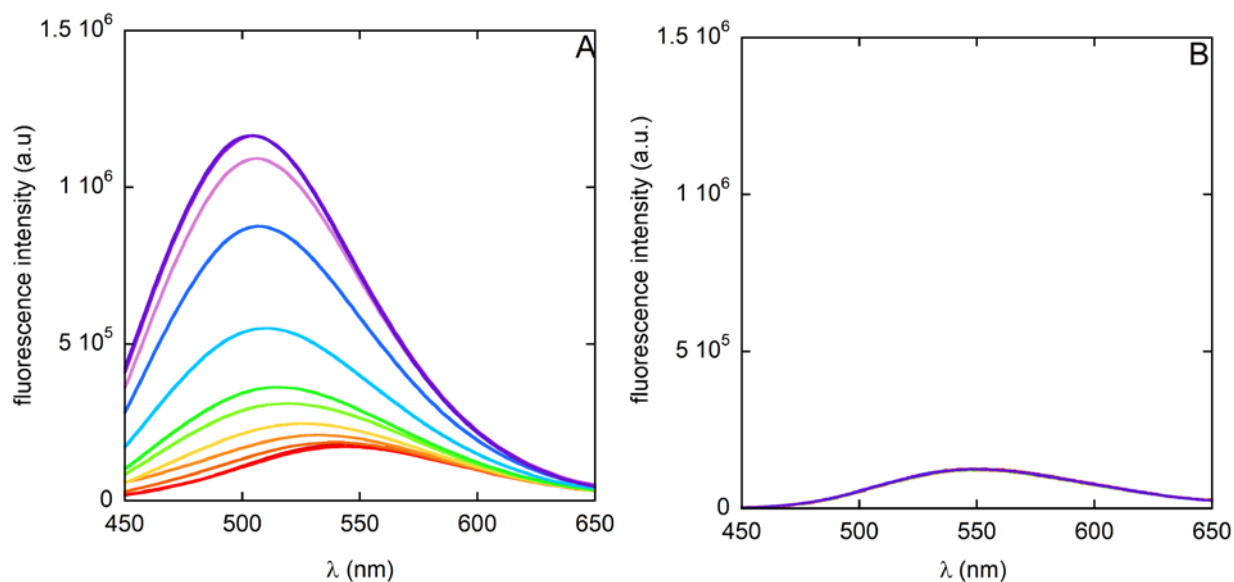


Figure 2. Effect of peptide/cell association on fluorescence spectra

A) Spectra of DNS-PMAP23 (50 μ M) in the presence of increasing *S. epidermidis* cell concentrations (0, 1×10^7 , 2×10^7 , 3.5×10^7 , 5.5×10^7 , 8.5×10^7 , 1×10^8 , 2×10^8 , 4×10^8 , 6×10^8 , 1.5×10^9 , 2×10^9 cells/mL).

B) Spectra of dansylamide (50 μ M) in the presence of increasing *S. epidermidis* cell concentrations (0, 2×10^7 ; 5.5×10^7 ; 8.5×10^7 ; 3×10^8 ; 6×10^8 ; 8.2×10^8 cells/mL).

Spectra are colored from red to violet with increasing cell concentration.

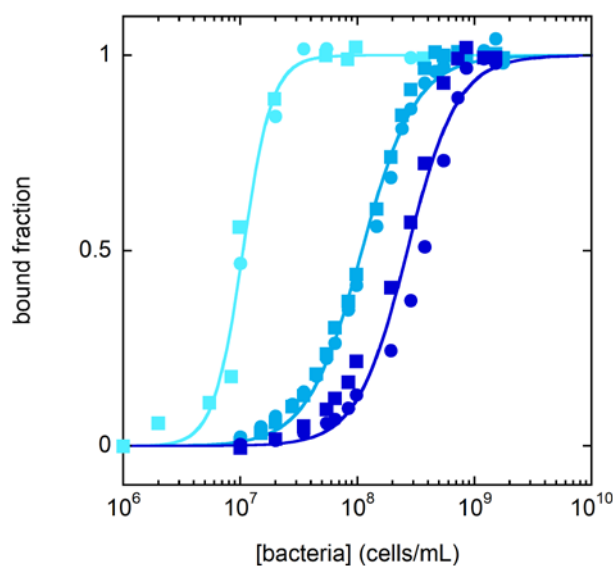


Figure 3. Binding of DNS-PMAP23 to *S. epidermidis* cells.

Cyan symbols: [DNS-PMAP23]= 2 μM. Light blue symbols: [DNS-PMAP23]= 10 μM. Blue symbols: [DNS-PMAP23]= 50 μM. Independent duplicate experiments are shown with different symbols.

In addition to providing a comparison of the affinities for Gram-positive and Gram-negative bacteria, the present data allow the calculation of the threshold of cell-bound peptide molecules needed for bacterial killing. Specifically, 3×10^6 molecules per cell are needed to start killing some bacteria, and 50×10^6 molecules are necessary for near-sterilization, as reported in Table 1. Again, the order of magnitude is similar to what has been observed previously with *E. coli* cells [Roversi 2014, Savini 2017].

S. epidermidis cells have a diameter between 0.5 and 1.5 μm, and thus a cell surface of 0.8-7 μm², or 1.6-14 μm² if both leaflets of the membrane are taken into account [Zhou 2015]. Considering an area of 5 nm² per DNS-PMAP23 molecule [Roversi 2014], the number of peptide molecules would largely exceed the total available membrane area (Table 1), more than previously observed for *E. coli*. In any case, the present findings generalize our previous results and the few literature data on peptide/cell association (reviewed in [Savini 2018]), demonstrating that a very high coverage of the cell surface by bound peptide molecules is necessary to cause bacterial killing in both Gram-negative and Gram-positive bacteria, and further support the relevance of the carpet model for pore formation in bacterial membranes.

Of course, our considerations leading to the conclusion that the threshold for bacterial killing is reached with a number of molecules corresponding to complete coverage of the cell surface, or even exceeding it, are based on strongly simplifying assumptions. The geometrical calculation of the membrane surface might provide an underestimation, due to the fact that local corrugations were not considered. More importantly, the peptides could bind to other cellular components, in addition to membrane lipids. Finally, we have considered peptide/cell association as an equilibrium process, but once pores are formed, the peptide can access intracellular molecules, to which it could bind as well.

The following sections address the question of where the high number of AMP molecules necessary for killing are located in the bacterial cell.

Table 1. Membrane coverage by DNS-PMAP-23 under the conditions of the bactericidal assay

Bacterium	[DNS-PMAP23] (μM)	Fraction of surviving bacteria (a)	C_{50} (cells/mL) (b)	Bound fraction (c)	Bound molecules/cell (d)	A_c/A_m (e)
<i>S. epidermidis</i> ATCC 12228 (Gram-positive)	2.0	0.91 \pm 0.02	(1.05 \pm 0.004) $\times 10^7$	1	(2.7 \pm 0.3) $\times 10^6$	1-8
	10	0.09 \pm 0.01	(1.09 \pm 0.02) $\times 10^8$	0.98 \pm 0.03	(13 \pm 1) $\times 10^6$	5-40
	50	(4 \pm 1) $\times 10^{-6}$	(2.7 \pm 0.1) $\times 10^8$	0.8 \pm 0.1	(50 \pm 10) $\times 10^6$	20-150
<i>E. coli</i> ATCC 25922 (Gram-negative) (f)	1.0	0.94 \pm 0.03	(9.0 \pm 0.9) $\times 10^7$	0.89 \pm 0.08	(1.2 \pm 0.2) $\times 10^6$	0.2
	10	(5 \pm 7) $\times 10^{-4}$	(1.8 \pm 0.2) $\times 10^8$	0.829 \pm 0.003	(11 \pm 1) $\times 10^6$	2

^aDetermined as the fraction of colony forming units (CFU) in a sample incubated for 2 h with DNS-PMAP23, as compared with the CFU of the control, i.e., $(4.5 \pm 0.5) \times 10^8$ cells/mL.

^bConcentration corresponding to half maximal binding (interpolated from the fitting curves).

^cDetermined at a cell density of $(4.5 \pm 0.5) \times 10^8$ CFU/mL, from the binding data.

^dCalculated from the peptide and cell concentration and the fraction of bound peptide.

^eRatio between the area covered by the bound peptides and the total area of the bacterial membrane. The reported values were calculated from the number of bound peptides per cell, assuming an area per DNS-PMAP23 molecule of 5 nm^2 [Roversi 2014], that each *S. epidermidis* cell corresponds to a sphere of 0.5-1.5 μm diameter [Zhou 2015], with two membrane leaflets, and that each *E. coli* cell corresponds to a cylinder of 1 μm diameter and 2 μm height [Schulz 2001], with four membrane leaflets.

^fData from [Roversi 2014] and [Savini 2017].

Where do the peptides bind? Role of lipoteichoic acid (LTA) in Gram-positive bacteria

The cell wall of most Gram-positive bacteria comprises teichoic acids (TA), highly charged anionic polymers [Malanovic 2016]. Several studies indicate that AMP bind strongly to lipoteichoic acid (LTA) [Malanovic 2015], and that this association may in fact reduce the total concentration of the peptide on the membrane interface [Malanovic 2016]. It should also be considered that LTA is released spontaneously into the culture medium during growth of Gram-positive bacteria [Soto 1996]. By contrast, peptidoglycan (the main component of the cell wall) is not negatively charged and therefore it is not considered to compete significantly with the membrane for interaction with AMPs [Malanovic 2016].

To verify the hypothesis of a relevant role of LTA in the association of DNS-PMAP23 with Gram-positive bacteria, peptide association to purified LTA was determined (Figure 4). Binding was observed, with a C_{50} of $8.0 \pm 0.3 \mu\text{M}$. To put this value in context, the content of LTA is 0.4-1.6% of the total cell dry weight [Huff 1982], which is $2-6 \times 10^{-12}$ g for Staphylococci [Cooper 1955]. Therefore, each cell contains $\sim 8-100 \times 10^{-15}$ g, or $10^{-16}-10^{-17}$ mol of LTA, and the C_{50} of 7 μM reported above corresponds roughly to the LTA concentration of a cell suspension with 10^8-10^9 cells/ml. Considering that, under the same conditions, we determined a C_{50} of $(1.09 \pm 0.02) \times 10^8$ cells/mL for the whole cells, the fraction of peptide molecules bound to LTA is likely significant.

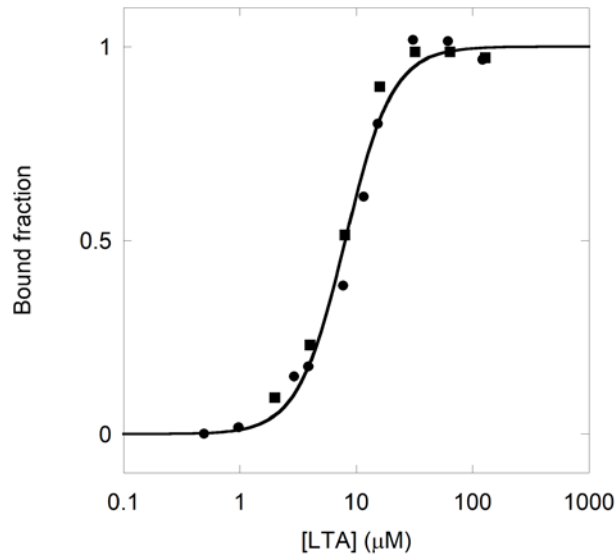


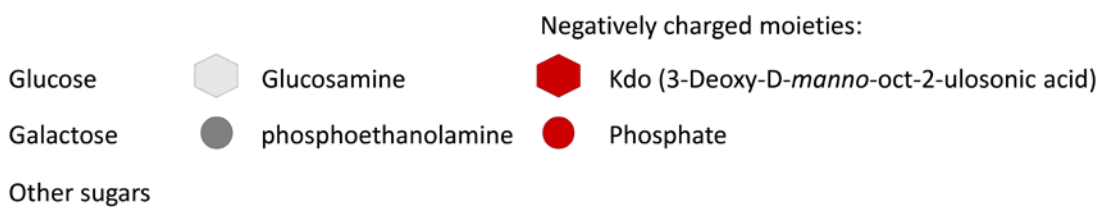
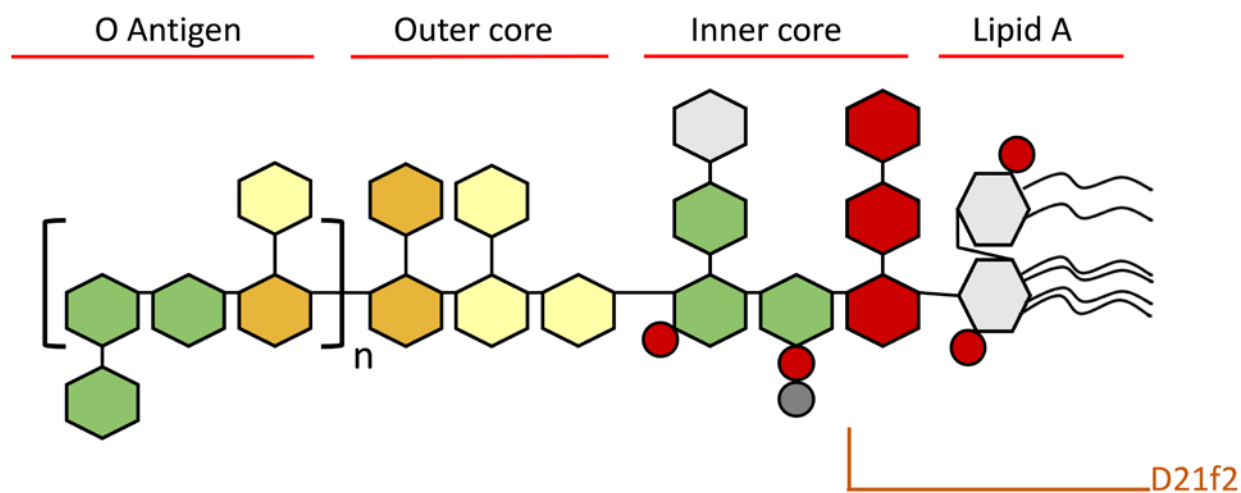
Figure 4. Binding of DNS-PMAP23 to LTA.

[DNS-PMAP23]= 10 μM. Independent duplicate experiments are shown with different symbols.

Where do the peptides bind? Role of LPS in Gram-negative bacteria

In the case of Gram-negative bacteria, an important component of the cell envelope is the LPS of the outer membrane. To investigate its role in peptide association to Gram-negative bacteria, we exploited *E. coli* strains with altered LPS structure.

D21 and D21f2 are two isogenic strains, except for the fact that D21f2 has a truncated LPS structure [Mangoni 2009]: as shown in Scheme 1, in D21f2 LPS comprises lipid A and Kdo (3-deoxy-D-manno-oct-2-ulsonic acid) only. The MIC values of DNS-PMAP23 against these bacterial strains are reported in Table 2, and show a fourfold increase in activity against the mutated D21f2 strain.



Scheme 1. Representation of lipopolysaccharide structure in *E. coli* bacterial strains. Adapted from [Ebbensgaard 2018] and [Gronow 2001].

Table 2. MIC and C_{50} values of DNS-PMAP23 against different *E. coli* strains.

	<i>E. coli</i> strain	MIC (μ M)	C_{50} (cells/mL)
LPS	D21	32	$(3.2 \pm 0.1) \times 10^8$
	D21f2	8	$(3.6 \pm 0.1) \times 10^8$
Anionic lipids	WT (K-12 MG1655)	32	$(4.0 \pm 0.1) \times 10^8$
	BKT12	8	$(3.0 \pm 0.1) \times 10^8$
	BKT29	8	$(2.4 \pm 0.1) \times 10^8$

[DNS-PMAP23] = 10 μ M (in the binding experiments).

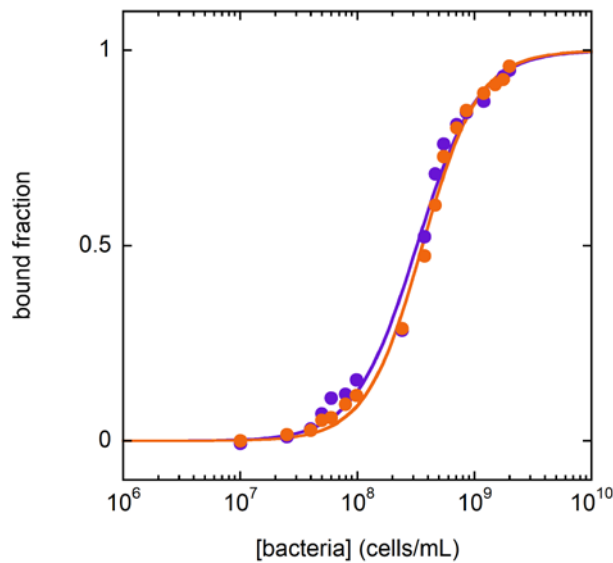


Figure 5. Binding of DNS-PMAP23 to *E. coli* strains with different LPS structures.
D21: purple; D21f2: orange. [DNS-PMAP23] = 10 μ M.

A higher activity against bacterial strains with a reduced LPS structure appears to be a rather general property of AMPs. Hansen and coworkers [Ebbensgard 2015, 2018] analyzed the activity of a collection of several AMPs (including cecropin B1, cecropin P1, melittin, indolicidin) on different *E. coli* mutant strains with a truncated LPS structure, observing that removal of the core region enhanced the activity of most peptides. In principle, these findings might have two possible explanations: the core region could bind strongly to the AMPs, reducing their effective concentration and precluding their association to and perturbation of the plasma membrane; alternatively, it might simply increase the stability of the outer membrane [Heinrichs 1998, Firdich 2005, Saar-Dover 2012] or the fitness of the bacteria might be reduced by the mutations leading to a truncated LPS [Yethon 2000].

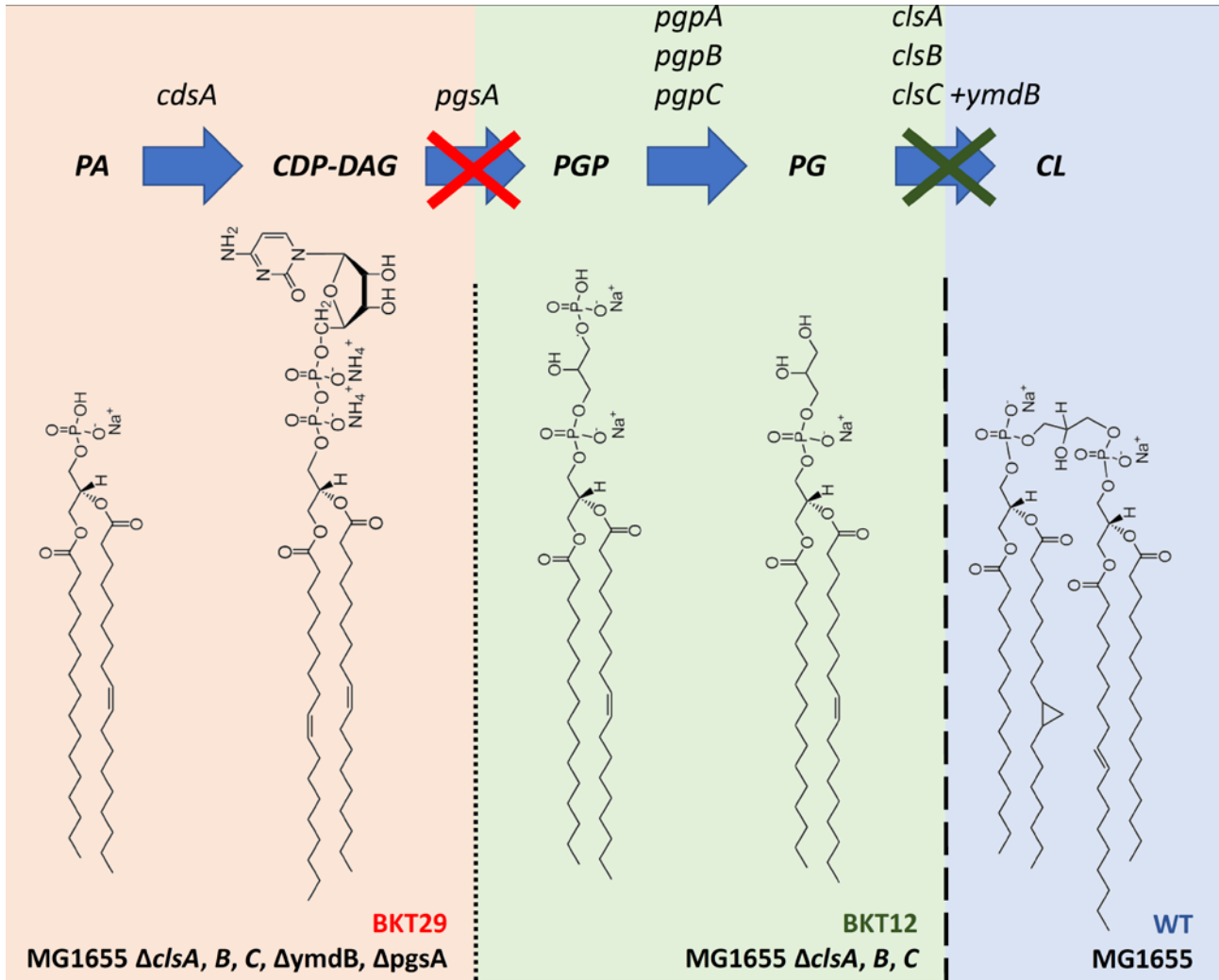
The interpretation based on strong peptide/LPS binding is supported by the antiendotoxin properties of many AMPs. The LPS released by Gram-negative bacteria in a severe infection can generate inflammation, leading to sepsis, and thus it is also called an endotoxin. AMP association to LPS can neutralize the inflammatory effects of these molecules [Brandenburg 2016], and a significant affinity of several AMPs for LPS has been reported [Larrick 1995, Nagaoka 2001, Bhunia 2007]. However, this property is not shared by all peptides, and several investigations indicate that the antimicrobial action of AMPs does not necessarily correspond to their anti-endotoxin activity [Brandenburg 2016]. In particular, PMAP-23 does not have an antiendotoxin activity [Veldhuizen 2017]. Indeed, experiments with purified LPS seem to rule out a significant interaction in the case of PMAP23. This peptide is unable to directly bind to purified LPS [Veldhuizen 2017] and preincubation with LPS does not inhibit its antimicrobial activity [Kim 2011]. However, the structure of aggregates of LPS, used in the biophysical studies or released by the bacteria and leading to activation of immune responses, is obviously extremely different from the way these molecules are presented on the surface of a cell [Brandebudg 2016; Richter 2011].

To verify peptide association to LPS in cells, we compared association of DNS-PMAP23 to D21 and D21f2 bacteria (Figure 5). No significant differences were observed, indicating that the O-antigen and the outer core of LPS do not play a significant role in the interaction of DNS-PMAP23 with bacterial cells. Our results confirm that the peptides mostly bind to the lipid component of the cellular envelope, as indicated by the shift of the emission spectrum to shorter wavelengths, caused by a decrease in the polarity of the fluorophore's environment. Therefore, the difference in peptide activity observed for the two strains supports the idea that LPS contributes to the structure and stability of the outer membrane.

Where do the peptides bind? Role anionic lipids

Based on studies on model membranes, the content in anionic lipids is generally considered a pivotal determinant of AMP activity and selectivity [Bobone 2019]. To verify this hypothesis in real cells, we exploited the BKT12 and BKT29 strains. As shown in Scheme 2, BKT12 lacks *clsA*, *B*, *C*, which are required for the synthesis of CL from PG. BKT29, in addition, lacks *pgsA*, which is essential for the synthesis of PG from its precursor (CDP-DAG, generated from PA).

Unexpectedly, peptide/cell binding was not significantly affected by the mutations; if anything, it was slightly enhanced (Figure 6). Z-potential measurements, performed in the presence of increasing concentration of the peptide, confirmed a very similar DNS-PMAP23/cell interaction for the two mutants BKT12 and BKT29 strains and the WT MG1655 (Figure 6). Finally, the mutant strains were even more susceptible to DNS-PMAP23 than the WT, as reported in Table 2. All these findings are very surprising, considering the well-known relevance of electrostatic interactions for the association of AMPs with bacterial membranes.



Scheme 2. PG and CL biosynthesis

Enzymatic steps in the bacterial synthesis of cardiolipin. The acronyms indicated on top correspond to the genes coding for the following proteins:

cdsA: cytidine diphosphate (CDP) diacylglycerol synthase A; *pgsA*: phosphatidylglycerophosphate synthase A; *pgpA*, *B*, *C*: phosphatidylglycerol synthases; *clsA*, *B*, *C*: cardiolipin synthases; *ymdB*: O-acetyl-ADP-ribose deacetylase.

PA= phosphatidic acid; CDP-DAG=cytidine-diphosphate-diacylglycerol; PGP= phosphatidyl glycerophosphate; PG= phosphatidyl glycerol; CL=cardiolipin.

Dotted and dashed lines indicate the enzymes missing in the BKT29 and BKT12 mutant strains.

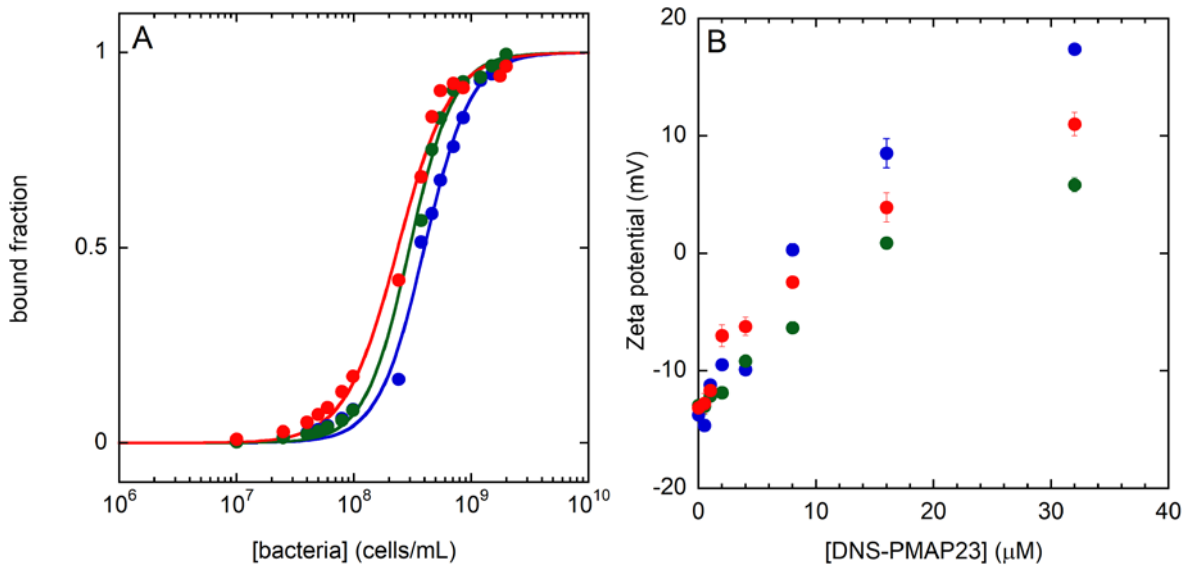


Figure 6. Binding of DNS-PMAP23 with *E. coli* strains lacking CL or PG and CL, compared to the WT strain.
 A) Fraction of DNS-PMAP-23 bound to different *E. coli* strains. [DNS-PMAP23] = 10 μM.
 B) Zeta-potential measurements of different *E. coli* strains (1×10^7 CFU/mL) in the presence of increasing peptide concentrations.
 WT (K-12 MG1655): blue; BKT12: green; BKT29: red.

Lipidomic studies provided an explanation for our unexpected findings. The content of PG, CL and of their anionic precursor phosphatidic acid (PA) were analyzed. As shown in Figure 7, BKT12 bacteria have a higher content of CL precursor PG, while in the BKT29 strain the content of PG precursor PA is enhanced. As a consequence of these modifications in lipid content, the overall charge of the membrane in the three strains might be very similar, as indicated by our binding and Z-potential measurements. These findings are consistent with results reported on similar mutated strains. For instance, strain UE54, which lacks CL and PG like our BKT29, was demonstrated to have an enhanced PA content [Mileykovskaya 2009, Oliver 2014]. Similarly, in a BKT12 strain derived from a different WT than ours [Tan 2012], depletion of CL in BKT12 was compensated by PG, so that the total % of anionic lipids stayed essentially constant.

The higher susceptibility of the mutant strains to DNS-PMAP23 (which is not due to a significant difference in binding) can be easily explained by the drastic effects of the gene deletions on the fitness of the bacteria [Shiba 2004]. Interestingly, our data on the PG and CL mutants demonstrate how difficult it is for the bacteria to modify the charge properties of their membranes.

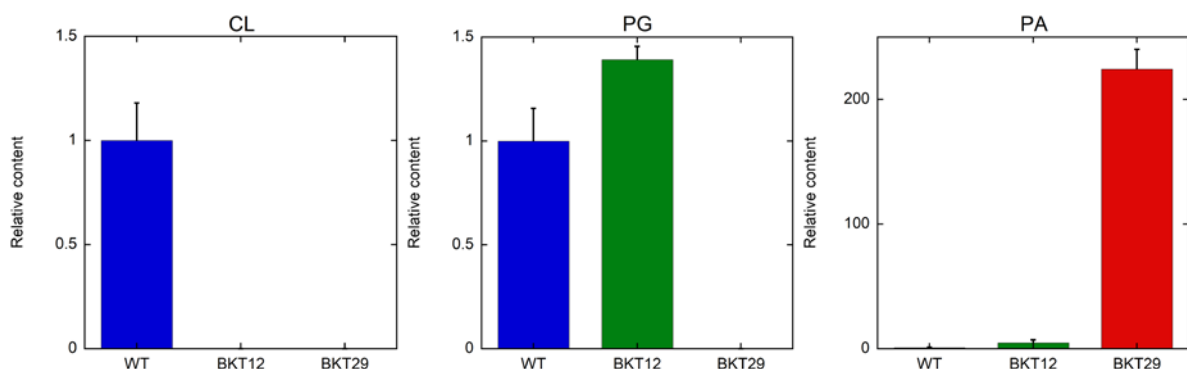


Figure 7. Content of CL, PG and PA in different *E. coli* strains.
 The lipid contents are reported after normalization to the WT strain.

Where do the peptides bind? Association to live and dead bacteria

In our binding studies, we titrate the peptide with live bacterial cells. However, after pore formation, the peptide has access to the intracellular contents, with several additional anionic molecules available for binding [Zhu 2019].

Recently, AMP accumulation inside bacterial cells after membrane perturbation and bacterial killing has been observed in three microscopy studies [Snoussi 2018, Zhu 2019, Wu 2019]. Compared to single cell studies, our approach has the advantage of allowing a quantitative determination and direct comparison of peptide affinity to bacterial cells under different conditions.

We performed binding studies on sonicated bacterial cells for *E. coli* strains ATCC 25922, D21 and D21f2 (Figure 8 and Table 3). Our results clearly show that the affinity for dead bacteria is higher by approximately one order of magnitude. Therefore, peptide accumulation in dead cells is caused by the increased affinity, presumably due to the accessibility of internal components for binding, and it could be a general property of AMPs. For instance, PMAP23 binding to DNA has been previously reported [Baumann 2014] and association to nucleic acids is commonly observed for AMPs [Hale 2007].

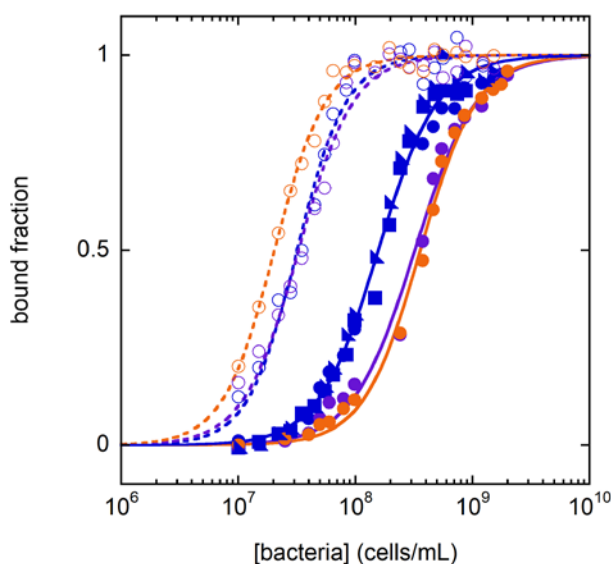


Figure 8. Binding of DNS-PMAP23 to live and dead *E. coli* cells.

ATCC 25922: blue; D21: green; D21f2: red. [DNS-PMAP23] = 10 μ M. Filled symbols and solid lines correspond to live bacteria, while empty symbols and dashed lines correspond to dead cells. Duplicate measurements are reported with different symbols.

Table 3. C_{50} values for live and dead *E. coli* cells.

<i>E. coli</i> strain	C_{50} (cells/mL)	
	Live	Dead
ATCC 25922	$(1.56 \pm 0.04) \times 10^8$	$(3.2 \pm 0.1) \times 10^7$
D21	$(3.2 \pm 0.1) \times 10^8$	$(3.3 \pm 0.1) \times 10^7$
D21f2	$(3.6 \pm 0.1) \times 10^8$	$(2.03 \pm 0.05) \times 10^7$

[DNS-PMAP23] = 10 μ M.

Conclusions

In this work, we have extended our previous studies on the quantitative determination of AMP binding to bacterial cells. Together with the determination of bacterial killing under the same conditions, these experiments provided several novel insights in the mechanism of action of AMPs.

We found that, for both Gram-negative and Gram-positive bacteria, $\sim 10^7$ AMP molecules must accumulate on a single cell to kill it. This number is supported from the few studies available in the literature, in addition to ours, using different techniques, AMPs and bacteria [Savini 2018]. In particular, here we extended its validity to Gram-positive microbes. Therefore, this finding seems to be of general relevance.

The huge amount of peptide molecules needed to cause cell death provides strong support to the carpet model for the mechanism of pore formation in bacterial membranes. Since this model was originally devised based on physico-chemical studies on artificial bilayers, its generalization to real cells underlines the importance of quantitative investigation of AMP-membrane interactions, and indicates that liposomes are a useful model to investigate the mechanism of action of AMPs, despite their simplicity. In particular, it had been argued that the bilayer coverage needed for pore formation in artificial membranes was too high to be reached at the concentrations needed for bacterial killing [Nicolas 2009]. On the contrary, our data demonstrate that the high affinity of AMPs for bacteria explains why this is actually happening under the conditions of *in vitro* assays [Savini 2017].

In the case of the Gram-positive bacteria studied here, the number of $\sim 10^7$ molecules even exceeds the total available surface area. Determination of the binding affinity of DNS-PMAP23 for LTA indicated that peptide association to this cellular component, and sequestration of a significant fraction of the peptide molecules, could explain this finding. By contrast, in the case of Gram-negative bacteria, the core region of LPS appears to have a marginal role in peptide binding, possibly providing a rationale for the lower membrane coverage needed in the case of those cells. On the other hand, we observed that truncation of the core portion increases the susceptibility of bacteria to AMP action, possibly due to the loss of the stabilizing effect of the saccharides on the structure of the outer membrane [Firdich 2005]. Our findings contribute to the ongoing debate on the role of LPS in the action of AMPs, indicating that stabilization of the outer membrane, rather than peptide sequestration, can explain its protective action [Ebbensgard 2018].

The anionic charge of bacterial membranes is generally considered one of the principal determinants of the selectivity of AMPs for pathogen versus host cells [Bobone 2011, 2019; Vaezi 2020]. However, this idea is based mainly on studies on artificial membranes. We tried to verify it in real bacteria by exploiting bacterial strains where the synthesis of PG and/or CL was blocked by specific mutations. Surprisingly, elimination of PG or of PG and CL did not cause a reduction in AMP/cell association. Lipidomic studies showed that this unexpected result was due to the compensation of the lacking lipids by other anionic membrane components. This finding underlines the difficulty involved in the development of bacterial resistance to AMPs by alteration of the membrane composition and charge.

Finally, our data showed that, once the cell membranes lose their integrity, AMP can access intracellular cell components and peptide/cell association increases by an order of magnitude. This finding provides a quantitative justification for the recent observation (by microscopy studies) of AMP accumulation in dead bacterial cells [Snoussi 2018, Zhu 2019, Wu 2019] and could be relevant to better describe bacterial population susceptibility to AMPs. Peptide sequestration by dead cells reduces the available peptide concentration and can thus protect the remaining bacteria from the action of AMPs [Snoussi 2018; Wu 2019]. Our result, by determining the affinity for both live and dead bacterial cells, can provide a basis for quantitative modeling of this effect [Yu 2018, Wu 2019]

Of course, several questions remain open regarding the interaction of AMPs with bacterial cells. The application of quantitative physico-chemical and biophysical approaches to studies of peptide/cell

association is a powerful tool for the characterization of AMPs that will hopefully lead to a step forward in our understanding of these molecules and in their development for therapeutic purposes.

Acknowledgements

We are very grateful to Prof. Karl Lohner (University of Graz) for his helpful contribution in designing the zeta potential and lipidomic studies reported in this article, which were performed in his laboratories. We also take this occasion to express our gratitude for his long-lasting friendship, scientific collaboration and for the inspiration that his research in peptide science and on biological membranes has provided over the years.

We thank Prof. J. C. Weisshaar (University of Wisconsin-Madison) for the kind gift of strains BKT12 and BKT29.

Financial support from the following institutions is kindly acknowledged: Italian Ministry of Education, University and Research (MIUR, grant PRIN 20157WW5EH_007, to LS), AIRC Foundation for Cancer Research in Italy (AIRC, grant IG19171, to LS), Sapienza University of Rome (grant RM11816436113D8A to MLM) and National Research Foundation of Korea (NRF, grant 2019R1A2B53070330 to YKP).

References

- Agrawal, A., Rangarajan, N., & Weisshaar, J. C. (2019). Resistance of early stationary phase *E. coli* to membrane permeabilization by the antimicrobial peptide Cecropin A. *Biochimica et Biophysica Acta (BBA)-Biomembranes*, 1861(10), 182990.
- Baumann, A., Démoulin, T., Python, S., & Summerfield, A. (2014). Porcine cathelicidins efficiently complex and deliver nucleic acids to plasmacytoid dendritic cells and can thereby mediate bacteria-induced IFN- α responses. *The Journal of Immunology*, 193(1), 364-371
- Bhunia, A., Domadia, P. N., & Bhattacharjya, S. (2007). Structural and thermodynamic analyses of the interaction between melittin and lipopolysaccharide. *Biochimica et Biophysica Acta (BBA)-Biomembranes*, 1768(12), 3282-3291.
- Bobone, S., Bocchinfuso, G., Park, Y., Palleschi, A., Hahm, K. S., & Stella, L. (2013). The importance of being kinked: role of Pro residues in the selectivity of the helical antimicrobial peptide P5. *Journal of Peptide Science*, 19(12), 758-769.
- Bobone, S., van de Weert, M., & Stella, L. (2014). A reassessment of synchronous fluorescence in the separation of Trp and Tyr contributions in protein emission and in the determination of conformational changes. *Journal of Molecular Structure*, 1077, 68-76.
- Bobone, S., & Stella, L. (2019). Selectivity of Antimicrobial Peptides: A Complex Interplay of Multiple Equilibria. In *Antimicrobial Peptides* (pp. 175-214). Springer, Singapore.
- Bocchinfuso, G., Palleschi, A., Orioni, B., Grande, G., Formaggio, F., Toniolo, C., ... & Stella, L. (2009). Different mechanisms of action of antimicrobial peptides: insights from fluorescence spectroscopy experiments and molecular dynamics simulations. *Journal of peptide science: an official publication of the European Peptide Society*, 15(9), 550-558.
- Bocchinfuso, G., Bobone, S., Mazzuca, C., Palleschi, A., & Stella, L. (2011). Fluorescence spectroscopy and molecular dynamics simulations in studies on the mechanism of membrane destabilization by antimicrobial peptides. *Cellular and molecular life sciences*, 68(13), 2281-2301.
- Boman, H. G., & Monner, D. A. (1975). Characterization of lipopolysaccharides from *Escherichia coli* K-12 mutants. *Journal of bacteriology*, 121(2), 455-464.
- Bortolotti, A., Wong, Y. H., Korsholm, S. S., Bähring, N. H. B., Bobone, S., Tayyab, S., ... & Stella, L. (2016). On the purported "backbone fluorescence" in protein three-dimensional fluorescence spectra. *Rsc Advances*, 6(114), 112870-112876.
- Brandenburg, K., Heinbockel, L., Correa, W., & Lohner, K. (2016). Peptides with dual mode of action: Killing bacteria and preventing endotoxin-induced sepsis. *Biochimica et Biophysica Acta (BBA)-Biomembranes*, 1858(5), 971-979.
- Casciaro, B., Calcaterra, A., Cappiello, F., Mori, M., Loffredo, M. R., Ghirga, F., ... & Quaglio, D. (2019). Nigritanine as a New Potential Antimicrobial Alkaloid for the Treatment of *Staphylococcus aureus*-Induced Infections. *Toxins*, 11(9), 511.
- CDC (2019) Antibiotic Resistance Threats in the United States, 2019. Atlanta, GA: U.S. Department of Health and Human Services, CDC.
- Cooper, P. D. (1955). The site of action of penicillin: some changes in *Staphylococcus aureus* during the first two hours growth in penicillin media. *Microbiology*, 13(1), 22-38.

- Di Grazia, A., Cappiello, F., Cohen, H., Casciaro, B., Luca, V., Pini, A., ... & Mangoni, M. L. (2015). D-Amino acids incorporation in the frog skin-derived peptide esculentin-1a (1-21) NH₂ is beneficial for its multiple functions. *Amino Acids*, 47(12), 2505-2519.
- Ebbensgaard, A., Mordhorst, H., Overgaard M.T., Nielsen CG, Aarestrup FM., & Hansen E.B. (2015). Comparative evaluation of the antimicrobial activity of different antimicrobial peptides against a range of pathogenic bacteria. *PlosOne*, 10(12):e0144611
- Ebbensgaard, A., Mordhorst, H., Aarestrup, F. M., & Hansen, E. B. (2018). The role of outer membrane proteins and lipopolysaccharides for the sensitivity of *Escherichia coli* to antimicrobial peptides. *Frontiers in microbiology*, 9.
- Farnaud, S., Spiller, C., Moriarty, L. C., Patel, A., Gant, V., Odell, E. W., & Evans, R. W. (2004). Interactions of lactoferricin-derived peptides with LPS and antimicrobial activity. *FEMS Microbiology Letters*, 233(2), 193-199.
- Freire, J. M., Domingues, M. M., Matos, J., Melo, M. N., Veiga, A. S., Santos, N. C., & Castanho, M. A. (2011). Using zeta-potential measurements to quantify peptide partition to lipid membranes. *European Biophysics Journal*, 40(4), 481-487.
- Fridrich, E., & Whitfield, C. (2005). Lipopolysaccharide inner core oligosaccharide structure and outer membrane stability in human pathogens belonging to the Enterobacteriaceae. *Journal of endotoxin research*, 11(3), 133-144.
- Gazit, E., Miller, I. R., Biggin, P. C., Sansom, M. S., & Shai, Y. (1996). Structure and orientation of the mammalian antibacterial peptide cecropin P1 within phospholipid membranes. *Journal of molecular biology*, 258(5), 860-870.
- Hale, J. D., & Hancock, R. E. (2007). Alternative mechanisms of action of cationic antimicrobial peptides on bacteria. *Expert review of anti-infective therapy*, 5(6), 951-959.
- Heinrichs, D. E., Yethon, J. A., & Whitfield, C. (1998). Molecular basis for structural diversity in the core regions of the lipopolysaccharides of *Escherichia coli* and *Salmonella enterica*. *Molecular microbiology*, 30(2), 221-232.
- Huff, E. (1982). Lipoteichoic acid, a major amphiphile of Gram-positive bacteria that is not readily extractable. *Journal of bacteriology*, 149(1), 399.
- Grieco, P., Carotenuto, A., Auriemma, L., Saviello, M. R., Campiglia, P., Gomez-Monterrey, I. M., ... & Mangoni, M. L. (2013). The effect of d-amino acid substitution on the selectivity of temporin L towards target cells: identification of a potent anti-*Candida* peptide. *Biochimica et Biophysica Acta (BBA)-Biomembranes*, 1828(2), 652-660.
- Gronow, S., & Brade, H. (2001). Lipopolysaccharide biosynthesis: which steps do bacteria need to survive?. *Journal of Endotoxin Research*, 7(1), 3-23.
- Huber, A., Oemer, G., Malanovic, N., Karl, L., Kovács, L., Salvenmoser, W., ... & Marx, F. (2019). Membrane sphingolipids regulate the fitness and antifungal protein susceptibility of *Neurospora crassa*. *Frontiers in Microbiology*, 10, 605.
- Kang, J. H., Shin, S. Y., Jang, S. Y., Kim, K. L., & Hahm, K. S. (1999). Effects of tryptophan residues of porcine myeloid antibacterial peptide PMAP-23 on antibiotic activity. *Biochemical and biophysical research communications*, 264(1), 281-286.
- Kim, J. Y., Park, S. C., Yoon, M. Y., Hahm, K. S., & Park, Y. (2011). C-terminal amidation of PMAP-23: translocation to the inner membrane of Gram-negative bacteria. *Amino acids*, 40(1), 183-195.

- Larrick, J. W., Hirata, M., Balint, R. F., Lee, J., Zhong, J., & Wright, S. C. (1995). Human CAP18: a novel antimicrobial lipopolysaccharide-binding protein. *Infection and immunity*, 63(4), 1291-1297.
- Luca, V., Stringaro, A., Colone, M., Pini, A., & Mangoni, M. L. (2013). Esculentin (1-21), an amphibian skin membrane-active peptide with potent activity on both planktonic and biofilm cells of the bacterial pathogen *Pseudomonas aeruginosa*. *Cellular and molecular life sciences*, 70(15), 2773-2786.
- Malanovic, N., Leber, R., Schmuck, M., Kriechbaum, M., Cordfunke, R. A., Drijfhout, J. W., ... & Lohner, K. (2015). Phospholipid-driven differences determine the action of the synthetic antimicrobial peptide OP-145 on Gram-positive bacterial and mammalian membrane model systems. *Biochimica et Biophysica Acta (BBA)-Biomembranes*, 1848(10), 2437-2447.
- Malanovic, N., & Lohner, K. (2016). Gram-positive bacterial cell envelopes: The impact on the activity of antimicrobial peptides. *Biochimica et Biophysica Acta (BBA)-Biomembranes*, 1858(5), 936-946.
- Mangoni, M. L., & Shai, Y. (2009). Temporins and their synergism against Gram-negative bacteria and in lipopolysaccharide detoxification. *Biochimica et Biophysica Acta (BBA)-Biomembranes*, 1788(8), 1610-1619.
- Marcellini, L., Borro, M., Gentile, G., Rinaldi, A. C., Stella, L., Aimola, P., Barra, D., Mangoni, M. L. (2009). Esculentin-1b(1-18)--a membrane-active antimicrobial peptide that synergizes with antibiotics and modifies the expression level of a limited number of proteins in *Escherichia coli*. *FEBS J*, 276(19), 5647-64.
- Matsuzaki, K (2019) Membrane permeabilization mechanisms. In *Antimicrobial Peptides* (pp. 9-16). Springer, Singapore.
- Matyash, V., Liebisch, G., Kurzchalia, T. V., Shevchenko, A., & Schwudke, D. (2008). Lipid extraction by methyl-tert-butyl ether for high-throughput lipidomics. *Journal of lipid research*, 49(5), 1137-1146.
- Melo, M. N., Ferre, R., & Castanho, M. A. (2009). Antimicrobial peptides: linking partition, activity and high membrane-bound concentrations. *Nature Reviews Microbiology*, 7(3), 245.
- Merlino, F., Carotenuto, A., Casciaro, B., Martora, F., Loffredo, M. R., Di Grazia, A., ... & Galdiero, M. (2017). Glycine-replaced derivatives of [Pro3, DLeu9] TL, a temporin L analogue: Evaluation of antimicrobial, cytotoxic and hemolytic activities. *European journal of medicinal chemistry*, 139, 750-761.
- Mileykovskaya, E., Ryan, A. C., Mo, X., Lin, C. C., Khalaf, K. I., Dowhan, W., & Garrett, T. A. (2009). Phosphatidic acid and N-acylphosphatidylethanolamine form membrane domains in *Escherichia coli* mutant lacking cardiolipin and phosphatidylglycerol. *Journal of Biological Chemistry*, 284(5), 2990-3000.
- Nagaoka, I., Hirota, S., Niyonsaba, F., Hirata, M., Adachi, Y., Tamura, H., & Heumann, D. (2001). Cathelicidin family of antibacterial peptides CAP18 and CAP11 inhibit the expression of TNF- α by blocking the binding of LPS to CD14+ cells. *The Journal of Immunology*, 167(6), 3329-3338.
- Nicolas, P. (2009). Multifunctional host defense peptides: intracellular-targeting antimicrobial peptides. *The FEBS journal*, 276(22), 6483-6496.
- Oliver, P. M., Crooks, J. A., Leidl, M., Yoon, E. J., Saghatelian, A., & Weibel, D. B. (2014). Localization of anionic phospholipids in *Escherichia coli* cells. *Journal of bacteriology*, 196(19), 3386-3398.
- Orioni, B., Bocchinfuso, G., Kim, J. Y., Palleschi, A., Grande, G., Bobone, S., ... & Stella, L. (2009). Membrane perturbation by the antimicrobial peptide PMAP-23: a fluorescence and molecular dynamics study. *Biochimica et Biophysica Acta (BBA)-Biomembranes*, 1788(7), 1523-1533.
- Pérez-Peinado, C., Dias, S. A., Domingues, M. M., Benfield, A. H., Freire, J. M., Rádis-Baptista, G., ... & Veiga, A. S. (2018). Mechanisms of bacterial membrane permeabilization by crotalidin (Ctn) and its fragment Ctn (15–34), antimicrobial peptides from rattlesnake venom. *Journal of Biological Chemistry*, 293(5), 1536-1549.

- Richter, W., Vogel, V., Howe, J., Steiniger, F., Brauser, A., Koch, M. H., ... & Brandenburg, K. (2011). Morphology, size distribution, and aggregate structure of lipopolysaccharide and lipid A dispersions from enterobacterial origin. *Innate immunity*, 17(5), 427-438.
- Roversi, D., Luca, V., Aureli, S., Park, Y., Mangoni, M. L., & Stella, L. (2014). How many antimicrobial peptide molecules kill a bacterium? The case of PMAP-23. *ACS chemical biology*, 9(9), 2003-2007.
- Saar-Dover, R., Bitler, A., Nezer, R., Shmuel-Galia, L., Firon, A., Shimoni, E., ... & Shai, Y. (2012). D-alanylation of lipoteichoic acids confers resistance to cationic peptides in group B streptococcus by increasing the cell wall density. *PLoS pathogens*, 8(9), e1002891.
- Savini, F., Luca, V., Bocedi, A., Massoud, R., Park, Y., Mangoni, M. L., & Stella, L. (2017). Cell-density dependence of host-defense peptide activity and selectivity in the presence of host cells. *ACS chemical biology*, 12(1), 52-56.
- Savini, F., Bobone, S., Roversi, D., Mangoni, M. L., & Stella, L. (2018). From liposomes to cells: Filling the gap between physicochemical and microbiological studies of the activity and selectivity of host-defense peptides. *Peptide Science*, 110(5), e24041.
- Schulz, H. N., & Jørgensen, B. B. (2001). Big bacteria. *Annual Reviews in Microbiology*, 55(1), 105-137.
- Seelig, J. (2004). Thermodynamics of lipid-peptide interactions. *Biochimica et Biophysica Acta (BBA)-Biomembranes*, 1666(1-2), 40-50.
- Shiba, Y., Yokoyama, Y., Aono, Y., Kiuchi, T., Kusaka, J., Matsumoto, K., & Hara, H. (2004). Activation of the Rcs signal transduction system is responsible for the thermosensitive growth defect of an *Escherichia coli* mutant lacking phosphatidylglycerol and cardiolipin. *Journal of bacteriology*, 186(19), 6526-6535.
- Snoussi, M., Talledo, J. P., Del Rosario, N. A., Mohammadi, S., Ha, B. Y., Košmrlj, A., & Taheri-Araghi, S. (2018). Heterogeneous absorption of antimicrobial peptide LL37 in *Escherichia coli* cells enhances population survivability. *eLife*, 7, e38174.
- Soto, A., Evans, T. J., & Cohen, J. (1996). Proinflammatory cytokine production by human peripheral blood mononuclear cells stimulated with cell-free supernatants of viridans streptococci. *Cytokine*, 8(4), 300-304.
- Starr, C. G., He, J., & Wimley, W. C. (2016). Host cell interactions are a significant barrier to the clinical utility of peptide antibiotics. *ACS chemical biology*, 11(12), 3391-3399.
- Steiner, H., Andreu, D., & Merrifield, R. B. (1988). Binding and action of cecropin and cecropin analogues: antibacterial peptides from insects. *Biochimica et Biophysica Acta (BBA)-Biomembranes*, 939(2), 260-266.
- Tan, B. K., Bogdanov, M., Zhao, J., Dowhan, W., Raetz, C. R., & Guan, Z. (2012). Discovery of a cardiolipin synthase utilizing phosphatidylethanolamine and phosphatidylglycerol as substrates. *Proceedings of the National Academy of Sciences*, 109(41), 16504-16509.
- Tran, D., Tran, P. A., Tang, Y. Q., Yuan, J., Cole, T., & Selsted, M. E. (2002). Homodimeric θ -Defensins from Rhesus macaque: Leukocytes Isolation, Synthesis, Antimicrobial Activities, and Bacterial Binding Properties of the Cyclic Peptides. *Journal of Biological Chemistry*, 277(5), 3079-3084.
- UN-IACG (2019). No Time to Wait—Securing the Future from Drug-resistant Infections. Report to the Secretary General of the United Nations.
- Vaezi, Z., Bortolotti, A., Luca, V., Perilli, G., Mangoni, M. L., Khosravi-Far, R., ... & Stella, L. (2020). Aggregation determines the selectivity of membrane-active anticancer and antimicrobial peptides: The case of killerFLIP. *Biochimica et Biophysica Acta (BBA)-Biomembranes*, 1862(2), 183107.
- van der Does, A. M., Hiemstra, P. S., & Mookherjee, N. (2019). Antimicrobial Host Defence Peptides: Immunomodulatory Functions and Translational Prospects. In *Antimicrobial Peptides* (pp. 149-171). Springer, Singapore.

- Veldhuizen, E. J. A., Scheenstra, M. R., Tjeerdma-van Bokhoven, J. L. M., Coorens, M., Schneider, V. A. F., Bikker, F. J, ... & Haagsman, H. P. (2017). Antimicrobial and immunomodulatory activity of PMAP-23 derived peptides. *Protein and peptide letters*, 24(7), 609-616.
- Wu, F., & Tan, C. (2019). Dead bacterial absorption of antimicrobial peptides underlies collective tolerance. *Journal of the Royal Society Interface*, 16(151), 20180701.
- Yethon, J. A., Gunn, J. S., Ernst, R. K., Miller, S. I., Laroche, L., Malo, D., & Whitfield, C. (2000). Salmonella enterica Serovar TyphimuriumwaaP Mutants Show Increased Susceptibility to Polymyxin and Loss of Virulence In Vivo. *Infection and immunity*, 68(8), 4485-4491.
- Yu, G., Baeder, D. Y., Regoes, R. R., & Rolff, J. (2018). Predicting drug resistance evolution: insights from antimicrobial peptides and antibiotics. *Proceedings of the Royal Society B: Biological Sciences*, 285(1874), 20172687.
- Zanetti, M., Storici, P., Tossi, A., Scocchi, M., & Gennaro, R. (1994). Molecular cloning and chemical synthesis of a novel antibacterial peptide derived from pig myeloid cells. *Journal of Biological Chemistry*, 269(11), 7855-7858
- Zasloff, M. (2019). Antimicrobial Peptides of Multicellular Organisms: My Perspective. In *Antimicrobial Peptides* (pp. 3-6). Springer, Singapore.
- Zhou, X., & Li, Y. (Eds.). (2015). *Atlas of Oral Microbiology: From Healthy Microflora to Disease*. Academic Press.
- Zhu, Y., Mohapatra, S., & Weisshaar, J. C. (2019). Rigidification of the Escherichia coli cytoplasm by the human antimicrobial peptide LL-37 revealed by superresolution fluorescence microscopy. *Proceedings of the National Academy of Sciences*, 116(3), 1017-1026.

Supplemental data to

Binding of an antimicrobial peptide to bacterial cells: interaction with different species, strains and cellular components.

F. Savini,^{1,*} M.R. Loffredo,^{2,*} C. Troiano,¹ S. Bobone,¹ N. Malanovic,³ T. O. Eichmann,⁴ L. Caprio,¹ V. C. Canale,¹ Y. Park,⁵ M. L. Mangoni,^{2,+} L. Stella^{1,+}

¹ Department of Chemical Science and Technologies, University of Rome Tor Vergata, Rome, Italy

² Laboratory affiliated to Pasteur Italia-Fondazione Cenci Bolognetti, Department of Biochemical Sciences, Sapienza University of Rome, Rome, Italy

³ Institute of Molecular Biosciences, Biophysics Division, Karl-Franzens University Graz, Graz, Austria.

⁴ Institute of Molecular Biosciences, Karl-Franzens University Graz and Center for Explorative Lipidomics, BioTechMed-Graz, Graz, Austria

⁵ Department of Biomedical Science, College of Natural Science, Chosun University, Gwangju, Republic of KOREA

* These authors contributed equally

+ to whom correspondence should be addressed

marialuisa.mangoni@uniroma1.it, stella@uniroma2.it

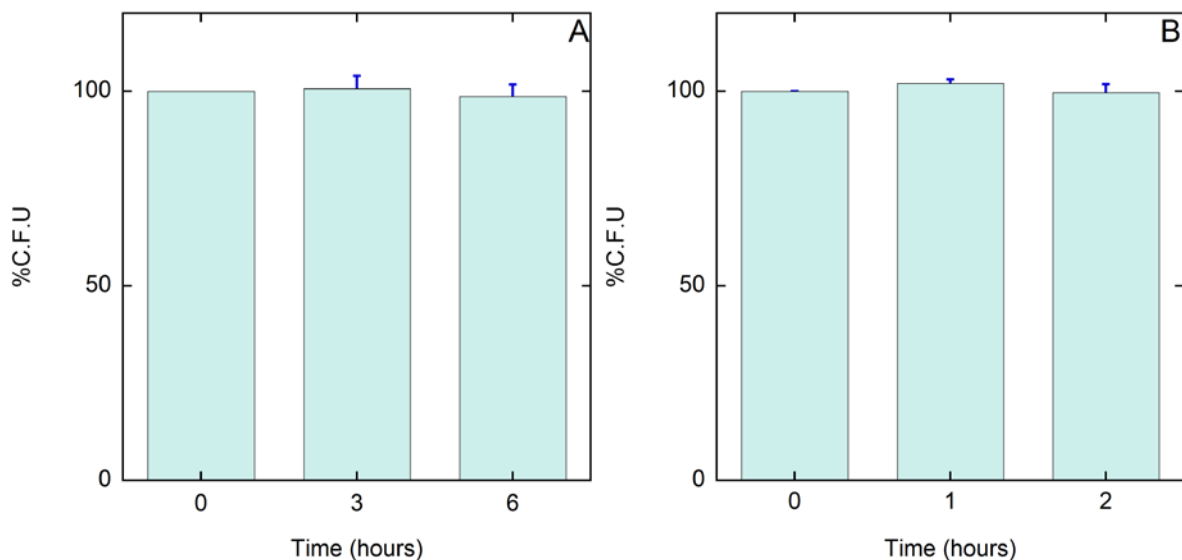


Figure S1. Survival of *S. epidermidis* cells in the minimal medium.

Percentage of viable bacterial cells after resuspension in buffer A, as a function of time. Temperature and starting cell density were set at 25 °C, 6×10^9 CFU/mL (panel A) and 37 °C, 4.5×10^8 CFU/mL (panel B).